Carbonatite complexes of the South Urals: geochemical features, ore mineralization, and geodynamic settings

Irina L. NEDOSEKOVA
Zavaritsky Institute of Geology and Geochemistry, Ural Branch of the Russian Academy of Sciences, Yekaterinburg, Russia

Abstract. The article presents the results of study of the Ilmeno-Vishnevogorsky and Buldym carbonatite complexes in the Urals. It has been established that the carbonatites of the Ilmeno-Vishnevogorsky complex are represented by high-temperature calciocarbonatites (sövites I and II) with pyrochlore ore mineralization. U-Ta-rich populations of uranium pyrochlores (I) and fluorocalciopyrochlores (II) crystallize in miaskite-pegmatites and sövites I; fluorocalciopyrochlores (III) and Sr-REE-pyrochlores (IV) of late populations form in sövites II. In the Buldym complex, along with high-temperature calciocarbonatites containing fluorocalciopyrochlore (III), medium-temperature varieties of magnesiocarbonatites with REE-Nb mineralization (monazite, niobo-aeschynite, columbite, etc.) are widespread. Miaskites and carbonatites of the Urals are characterized by high contents of LILE (Sr, Ba, K, Rb) and HFSE (Nb, Ta, Zr, Hf, Ti), which are close to the contents in rift-related carbonatite complexes of intraplate settings and significantly differ from synorogenic collisional carbonatite complexes. The Ural carbonatite complexes formed on continental rift margins during the opening of the Ural Ocean at the time of transition from extensional to compressional tectonics. Later on, they were captured and deformed in the suture zone as a result of collision. Plastic and brittle deformations, anatexis, recrystallization of rocks and ores of carbonatite complexes in the Urals are associated with orogenic and post-collision settings.

Keywords: linear carbonatites; deformed alkaline complexes; pyrochlore group minerals; Ilmeno-Vishnevogorsky and Buldym complexes; the Urals

Introduction. Large provinces of alkaline carbonatite magmatism are known in Russia. They are associated with rare metal deposits of various ore formation types. Thus, the provinces of ultramafic alkaline carbonatite complexes (UACC) with Na-type alkalinity are represented by the Karelian-Kola (the Baltic Shield), Maimecha-Kotui, East Sayan, Sette-Daban, and East Aldan (framing the Siberian Platform) provinces [1-3]. The complexes are on shields and in platform framing, where they form circular zonal plutons composed of alkaline rocks and carbonatites. Carbonatites of this type are enriched in Nb, Zr, Sr, rare earth elements (REE), Ba, V, Ti, P, Ta, Pb, Zn, Th. Large Nb-REE and Nb-P deposits, such as Tomtor (Yakutia) and Belaya Zima (Eastern Sayan), are associated with the carbonatites of the UACC complexes.

Carbonatite complexes of the alkaline-mafic formation with K-type alkalinity are confined to the rift structures of the platforms and are represented in Russia by the West Aldan province (Eastern Siberia) [3]. Alkali-gabbroid carbonatite complexes are also known in the folded regions: Altai-Sayan

and South Tien Shan (for example, Edelveis, Gorny Altai; Matcha complex, South Tien Shan), Western Transbaikalia (Vitim province [4]), in the Middle Timan (Chetlassky complex) [5]. Unlike the UACC complexes, Nb, Zr, P contents are low in them and only Sr, Ba, REE, V, Pb, Zn are concentrated. The largest REE deposits are associated with carbonatite complexes of the alkaline-mafic formation (for example, Mountain Pass, USA) [6].

Linear carbonatite complexes, an independent formational type of carbonatites associated with nepheline-syenite magmatism and/or linear zones of alkaline metasomatism, are located in the folded regions of the Urals and Siberia (Ilmeno-Vishnevogorsky, South Urals; Penchenga, Yenisei Ridge, Eastern Siberia) etc. [7, 8], and are also known in cratonic settings (Chernigovsky, Ukraine; Siilinjärvi, Finland). Commercial Nb deposits are associated with linear carbonatite complexes: Vishnevogorskoye, South Urals; Tatarka, Eastern Siberia.

The origin of linear carbonatite complexes and the associated Nb-Zr-REE mineralization is debatable. Since the rocks of the linear carbonatite complexes are deformed, it is assumed that they are earlier rift-related carbonatite complexes that were involved in the collision zone [9]. However, some researchers suggest that these complexes formed at the orogenic stage of the folded areas development [10, 11, 12]. For carbonatite complexes of the Urals, the rift-related [13], crustal anataxis [14, 15], metamorphogenic [16], and subduction [17] formation models are discussed.

The article presents the results of geochemistry, petrochemistry, and ore mineralization study of linear carbonatite complexes from the South Urals (Ilmeno-Vishnevogorsky miaskite-carbonatite and Buldym ultramafic carbonatite complexes). The petro- and geochemical features, PT conditions for the formation of carbonatites, and features of the composition and evolution of ore minerals are discussed. Carbonatite complexes of the Urals are compared with intraplate rift-related carbonatite and deformed carbonatite complexes (DARC) of various geodynamic settings. Based on the data obtained, we propose a geodynamic model for the formation of carbonatite complexes in the Urals.

Geological characteristics of carbonatite complexes of the Urals. The Ilmeno-Vishnevogorsky (IVC) and Buldym carbonatite complexes are in the South Urals, within the East Ural collisional megazone, near the giant suture zone, the Main Uralian Fault, and occur in the anticlinal structure of the Sysert-Ilmenogorsky block (or terrane, microcontinent), composed by the Archean-Proterozoic continental complexes. The base of the block is composed of the Selyankino sequence rocks: Archean gneiss-granulites and migmatites (AR), Mesoproterozoic amphibolites and plagiogneisses with calciphyre and marble interbeds (PR_1); in the framing, Middle Riphean gneiss-amphibolite and quartzite-schist strata (Rf_2) are occurred. The block is separated from the Main Uralian Fault zone by a fault along which gabbro-ultramafic massifs (O_1) are located, associated with island-arc volcanic-sedimentary complexes (D_2). Paleozoic collisional (360-320 Ma) and postcollisional (260-250 Ma) granitic magmatism is widespread in all structures of the block [18].

The Ilmeno-Vishnevogorsky complex intrudes the Archean-Proterozoic rocks of the Selyankinskaya sequence and forms two large massifs of nepheline syenites located in the anticlinal dome, as well as an extended linear zone of near-meridional strike in the anticlinal axis. Ultramafic massifs of the Buldym complex (Buldym, Spirikhinsky, Khaldikhinsky, etc.) form lenticular bodies with linear zones of alkaline metasomatic rocks and carbonatites framed by miaskite intrusions (see Fig.1 from I.L.Nedosekova, S.V.Pribavkina, Ore niobium minerals of the pyrochlore group from carbonatite complexes of the Urals: compositional features and geochemical evolution. *Izvestiya USMU.* 2019. Iss. 3(55), p. 46-57).

According to U-Pb, Sm-Nd, and Rb-Sr dating, the IVC and Buldym complexes of the South Urals formed in the Paleozoic (O_3-S). Rb-Sr whole-rock isochrone of miaskites showed the age of 446±13 Ma [13] for the Ilmenogorsky massif and 438±8 Ma [19] for the Vishnevogorsky massif. The U-Pb age of miaskite zircons is 434±15 Ma (Ilmenogorsky massif) and 417±5 Ma [20] (Vishnevogorsky massif). A close U-Pb age of 432±1.5 Ma was obtained for zircons from ultramafic rocks of the Buldym complex [21]. IVC carbonatites were dated at 432±12 [22], 419±20 [23], and

417±3 Ma [24] (U-Pb method, zircons). A younger age, 388±52 Ma (D$_2$), was obtained for carbonatites by the Sm-Nd method [17]. Moreover, geochronological data (mineral Rb-Sr isochrones, U-Pb age of late generations of zircons) register later processes of rocks alteration of the IVC and Buldym complexes at the collisional (~320-280 Ma) [24, 25] and postcollisional (~250-240 Ma) [13, 26, 27] stages of the Ural folded region evolution.

The Ilmeno-Vishnevogorsky complex consists of two intrusive massifs of K-Na plumasite nepheline syenites (miaskites), Vishnevogorsky and Ilmenogorsky (20-25 × 6 km), connected by the Central Alkaline Band (CAB), more than 100 km long and composed of sheet-like bodies of miaskites, syenites, glimmerite-like rocks, carbonatites, and fenites. Miaskites are deformed to varying degrees and are represented by fine- and medium-grained gneissic, taxitic, pegmatoid, and porphyritic varieties. In the CAB, sheet-like and lenticular bodies of miaskites alternate with interbeds of glimmerite-like (calcite-amphibole-micaceous) rocks, carbonatites, syenites, and fenites. They occur subconformably with the schistosity of the host rocks, often interstratified, deformed, and cataclastic.

Miaskite-pegmatites (nepheline-feldspar, nepheline-cancrinite-feldspar) and syenite-pegmatites (biotite-feldspar, pyroxene-feldspar) form vein bodies 50-300 m long and to 10 m thick. Syenite-pegmatites occur mainly in fenites and syenites, as well as at rock contacts. Miaskite-pegmatites are widely developed both in miaskite massifs and in fenite aureole. The bodies of miaskite-pegmatites are often subconformable with the deformation banding of miaskites or form vein bodies with apophyses crossing the banding. Veins of miaskite-pegmatites have complex structure: in the edges – nepheline-biotite-microcline aggregate, the central parts of the block structure are composed of nepheline, microcline, albite, sometimes cancrinite, less often, calcite aggregate, with biotite, fluorapatite, ilmenite, zircon, pyrochlore. Accessory minerals in miaskite-pegmatites include magnetite, thorite, thorianite, yttrialite-(Y), ferrocolumbite, fergusonite-(Ce), rutile, fluorite, and corundum [28].

Carbonatites form sheet-like and vein bodies (to 10 m thick, hundreds of meters long) in the apical part of the Vishnevogorsky massif, in the CAB rocks, and also occur as veins and stockworks in fenite aureoles of miaskite intrusions. Early carbonatites (sövites I) are predominantly developed in the miaskites of the CAB and are represented by silicocarbonatites: fluidal, aphanitic, taxitic varieties, often brecciated and cataclastic, of calcite composition, containing nepheline, K-feldspar, biotite, sometimes pyroxene, albite, accessory black uranium pyrochlore and rarely brown pyrochlore (with black pyrochlore nuclei), ilmenite, apatite, zircon, magnetite, pyrrhotite, pyrite. Brecciated sövites contain round fragments (1-5 cm) of host rocks (miaskites or fenites) and large grains of their minerals, cemented by a fine-grained albite-biotite-calcite groundmass.

Late carbonatites (sövites II) are widely represented in the apical part of the Vishnevogorsky massif, forming vein-like bodies subconformable to the massif contacts and miaskite banding. Sövites II are leucocratic, coarse-grained, with a banded distribution of silicate and accessory minerals, contain large (to 10-20 cm) crystals of biotite, apatite, albite, red-brown pyrochlore (sometimes with dark pyrochlore cores), ilmenite, zircon, magnetite, pyrrhotite, pyrite. In fenites, vein and stockwork-like calcite carbonatites contain aegirine-augite, orthoclase, biotite, apatite, titanite, red pyrochlore, ilmenite, magnetite, pyrrhotite, pyrite, zircon, monazite, orthite, and chevkinite.

The Buldym ultramafic carbonatite complex consists of the Buldym, Spirikhinsky, and Khaldikhinsky massifs composed of metadunites, metaolivinites, olivine-enstatite rocks and linear zones of alkaline metasomatic rocks and carbonatites containing REE-Nb mineralization [14, 29]. Massifs of ultramafic rocks occur among the Lower Proterozoic (PR$_1$) amphibolites, plagiogneisses, and schists framed by the Vishnevogorsky and Ilmenogorsky miaskite intrusions.

Carbonatites in ultramafic rocks form extended zones of vein development, accompanied by carbonate-phlogopite-richterite, phlogopite-richterite and phlogopite metasomatic rocks. Carbonatites are coarse-grained (to giant-grained), with a banded distribution of silicate and accessory minerals parallel to the bodies contacts. Early carbonatites are dolomite-calcite (sövites III) and contain amphiboles of the richterite-magnesioarfvedsonite series, micas of the phlogopite-tetraferriflogopite

series, accessory red-brown pyrochlore, ilmenite, magnetite, pyrrhotite, pyrite, and zircon [29]. Dolomitic carbonatites (beforsites IV) contain tetraferriflogopite, amphibole (winchite-cataphorite series), chlorite, Nb-REE mineralization represented by monazite-(Ce), aeschinite-(Ce), columbite, orthite-(Ce), thorite, fergusonite-(Ce), bastnaesite-(Ce), chromognesiochevkinite-(Ce), chromic davidite-(Ce). Strontianite, ilmenorutile, and molybdenite are also known in them [29, 30].

Deposits and ore occurrences of Nb, Zr, and REE are associated with pegmatites and carbonatites of the IVC and Buldym complexes. The largest Nb deposits are in the zone of endo- and exocontact of the Vishnevogorsky miaskite intrusion. The Vishnevogorsky deposit, which was discovered in the 1940s and has been developed for more than 50 years, is associated with pyrochlore-containing carbonatites and pegmatites. It is confined to the northwestern endocontact of the Vishnevogorsky miaskite massif (ore zone 147, length 4 km) and saddle-shaped miaskite deposit (ore zone 140, length 1.7 km). Separate zones of the Vishnevogorsky deposit are in the exocontact of the Vishnevogorsky massif (ore zones 125 and 135) and are associated with carbonatites and syenite-pegmatites in a fenite aureole.

Deposits and ore occurrences of pyrochlore-bearing carbonatites are located in the CAB. The Potanino Nb deposit is the largest one. It is confined to the stockwork zone of carbonatites (length 15 km, thickness 40 m) at the eastern contact of miaskite intrusions with a fenite aureole. The Svetloozerskoye, Uvildy, Baidashevo, and Ishkul ore occurrences of pyrochlore-bearing carbonatites are also known [14].

The Buldymskoye and Spirikhinskoye deposits and the Khaldikhinskoye ore occurrence of Nb and REE associated with carbonatites in the cognominal ultramafic massifs of the Buldym complex were discovered and explored in the 1980s [14]. Ore occurrences of carbonatites with Nb-REE mineralization were found in the ultramafic massifs of the Kagansky and Silachsky complexes [14]. In the framing of the Ilmenogorsky miaskite massif, ore occurrences of Nb-REE carbonatites are also known in ultramafic rocks (mine 97, Ilmenskoye ore occurrence) [30].

Methodology. The petrogenic elements in the rocks of the carbonatite complexes from the Urals (24 samples) were analysed by wet chemistry and X-ray diffraction methods at the Institute of Geology and Geochemistry, Ural Branch of the Russian Academy of Sciences in Yekaterinburg. Rare-earth and rare elements were determined using ICP-MS analysis on a high-resolution tandem analyzer with ionization in inductively coupled plasma HR-ICP-MS Element2 (IGG UB RAS, Yekaterinburg). The error of multi-element analysis does not exceed 8-10 % if the element content is 10-20 times greater than its detection limit.

The chemical composition of ore rare-metal Nb-minerals of the pyrochlore group was studied using the Cameca-100 microprobe at the IGG UB RAS (CUC "Geoanalitik", analysts D.V.Zamyatin and V.Bulatov) and using the CAMEBAX electron microprobe at the IGM SB RAS in Novosibirsk (analyst V.V. Sharygin). The following standards were used: apatite (F, P), jadeite (Na), rhodonite (Mn), orthoclase (K), $CaSiO_3$ (Ca, Si), TiO_2 (Ti), Fe_2O_3 (Fe), ThO_2 (Th), UO_2 (U), PbS (Pb), Nb, Ta, $SrSO_4$ (Sr), $BaSO_4$ (Ba), Al_2O_3 (Al) and REE-doped aluminosilicate glasses (La, Ce, Y, Sm, Pr, Nd). Pyrochlores were analyzed at an accelerating voltage of 15 kV and an electron probe current of 40 nA using crystal analyzers: TAP, LPC0, LPET, PET, LIF. The pulse accumulation time at the peak maximum was chosen from 10 to 30 s. The detection limits for F, Fe, Mn, Ti, Pb, La, Y were 0.075-0.1 wt.%; Sr, U, Nb, Sm, Ce, Pr, Nd, Ta – 0.15-0.2 wt.%; Na, Al, Si, P, Ca, Ba, Th < 0.05 wt.%.

Using scanning electron microscopy, images of micro-objects were obtained. Their composition was analysed by a Jeol JSM-6390LV (JEOL) scanning electron microscope with an INCA Energy 450 X-Max 80 (Oxford Instruments) energy dispersive spectrometer (CUC "Geoanalitik", IGG UB RAS, I.A.Gottman).

Petrochemical characteristics, geochemical features, and PT-conditions for the formation of rocks of the Ilmeno-Vishnevogorsky and Buldym complexes. Representative chemical compositions and contents of rare elements in the rocks of the IVC and Buldym complexes are shown in Tables 1-3 and in Fig.1.
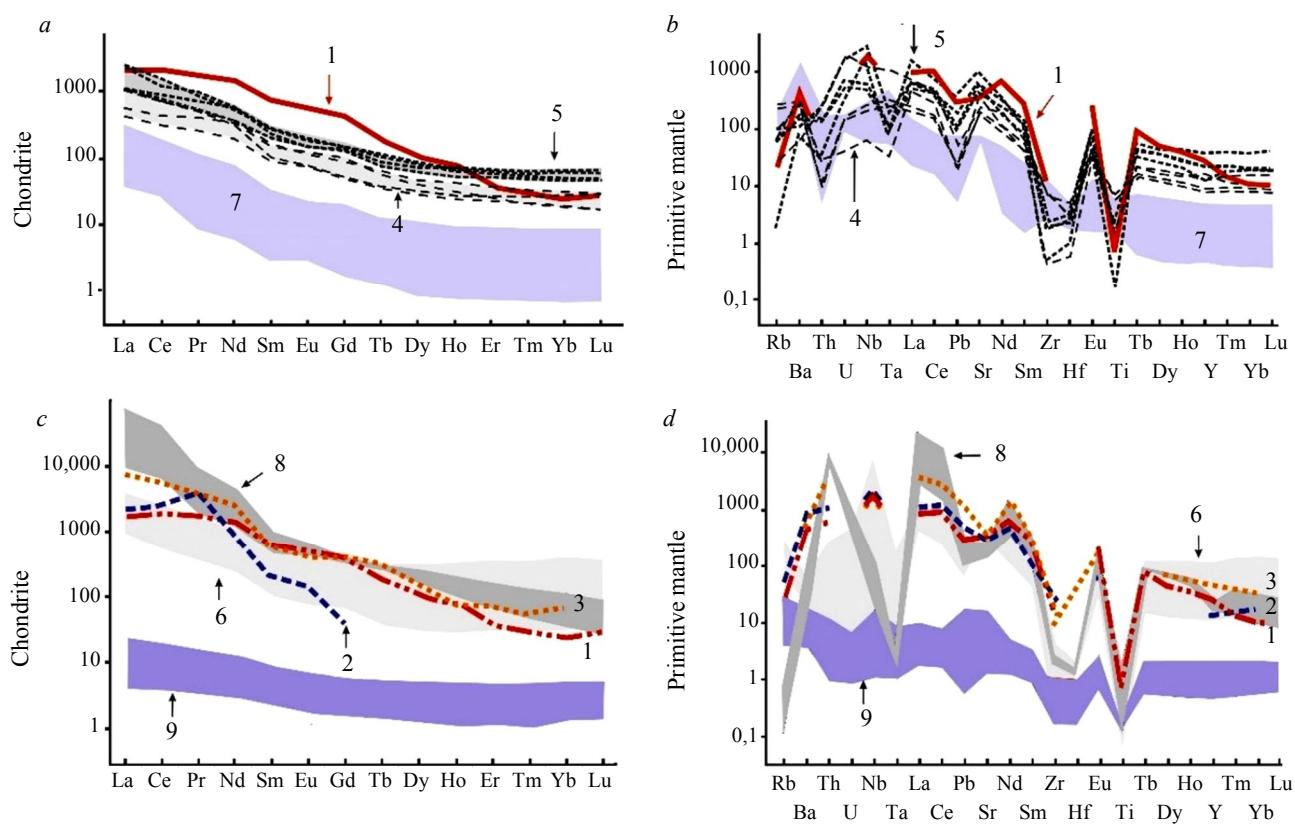
Fig.1. Chondrite-normalized REE contents and spider diagrams for the IVC (*a, b*) and Buldym complex (*c, d*) rocks, South Urals

1 – intermediate calciocarbonatite (Wooley and Kempe, 1989); 2 – intermediate magnesiocarbonatite (Wooley and Kempe, 1989);
3 – ferrocarbonatite [31]; 4 – sövite I (IVC); 5 – sövite II (IVC); 6 – sövite III (Buldym); 7 – miaskites (IVC); 8 – beforsites
(Buldym massif); 9 – ultramafic rocks (Buldym)

Table 1

Representative chemical compositions of the IVC miaskites

Mineral	Sample (sample N)						
	324 (1)	323 (2)	337 (3)	338 (4)	Sav4 (5)	Po-4 (6)	Peg2 (7)
SiO_2, wt.%	53.62	51.03	57.69	53.62	57.51	53.63	51.38
TiO_2	0.58	0.57	0.40	0.67	1.24	0.43	0.04
Al_2O_3	20.98	22.75	21.55	18.45	17.55	20.29	27.37
Fe_2O_3	1.64	0.91	1.25	1.43	1.90	1.42	0.16
FeO	1.95	2.25	1.05	2.10	3.2	1.4	0.4
MnO	0.16	0.12	0.05	0.09	0.21	0.07	0.02
MgO	0.96	0.88	0.55	1.03	1.57	0.72	0.16
CaO	2.21	2.22	1.02	3.95	2.80	3.11	0.89
Na_2O	6.60	8.00	6.20	6.00	5.8	9.7	12.40
K_2O	7.97	7.50	7.14	7.62	5.66	5.15	5.22
P_2O_5	0.23	0.19	0.02	0.10	0.24	0.04	0.02
LoI	2.5	2.70	2.0	3.5	1.8	2.7	1.5
Σ	99.45	99.10	98.91	98.61	99.48	98.67	99.56
Li, ppm	9	7	2.1	5	32	2.2	1.9
Rb	59	44	34	42	114	55	48
Sr	2317	1902	1661	2530	1405	1647	400
Ba	1816	1592	5667	9857	1589	2406	70
Sc	1.61	1.00	1.25	1.36	2.5	0.96	0.17
V	179	159	194	100	78	69	3.4
Cr	93	162	84	70	8	4	5
Co	0.41	0.10	1.6	3.7	9	7	0.5
Ni	1.07	0.56	16	1.8	9	7	1.9

End of Table 1

Mineral	Sample (sample N)						
	324 (1)	323 (2)	337 (3)	338 (4)	Sav4 (5)	Po-4 (6)	Peg2 (7)
Cu	0.33	14	7	8	34	30	2
Zn	61	22	22	64	87	25	5
Y	10	8	2.1	11	20	6	0.3
Nb	57	69	45	51	188	54	120
Ta	2.4	3.9	2.1	3.6	20	4.3	2
Zr	94	335	109	144	77	40	42
Hf	1.52	5	0.78	0.95	1.30	0.71	0.9
Pb	2.6	2	0.94	1.45	12	2.07	1.6
Th	1.66	2	0.32	0.85	13	1.43	0.52
U	1	8	1.7	2.1	3.2	2.4	0.18
La	105	69	15	40	80	23	0.6
Ce	162	107	28	77	142	35	1.3
Pr	15	10	1.30	8.05	17	4.51	0.14
Hd	41	30	4.35	27	57	15	0.51
Sm	4.76	3.78	0.66	3.92	7.62	2.17	0.08
Eu	1.27	1.03	0.26	1.91	2.01	0.87	0.05
Gd	3.16	2.51	0.55	2.95	6.14	1.75	0.08
Tb	0.40	0.33	0.07	0.40	0.69	0.21	0.01
Dy	1.93	1.72	0.35	1.99	4.17	1.26	0.07
Ho	0.35	0.31	0.07	0.40	0.79	0.25	0.02
Er	0.96	0.86	0.20	1.05	2.25	0.69	0.06
Tm	0.13	0.12	0.03	0.14	0.33	0.10	0.01
Yb	0.80	0.78	0.18	0.85	2.15	0.69	0.09
Lu	0.12	0.12	0.03	0.13	0.31	0.11	0.02
ΣREE + Y	350	236	53	178	342	92	3.34
K_{agp}	0.93	0.94	0.83	0.98	0.89	1.06	0.95
K/Na, mol.	0.79	0.62	0.76	0.84	0.64	0.35	0.28
(La/Yb)n	89	59	51	31	25	23	4
Y/Ho	25	26	21	28	25	24	17
Eu/Eu*	0.96	0.96	1.48	1.64	0.87	1.32	1.99

Note. 1-4 – miaskites of the Vishnevogorsky massif: 1, 2 – fine- and coarse-grained mesocratic miaskites of the apical part of the massif; 3, 4 – gneissic leucocratic and mesocratic miaskites of the root part of the massif; 5 – miaskite of the Ilmenogorsky massif; 6 – antiperthite miaskite of the CAB; 7 – miaskite-pegmatite (Vishnevogorsky massif); K_{agp} – (Na + K)/Al, mol.

Table 2

Representative chemical compositions of the IVC carbonatites

Mineral	Sample (sample N)							
	LPo1 (1)	354 (2)	D11-3 (3)	Z-2 (4)	LPo2 (5)	Po-6 (6)	331 (7)	V348 (8)
SiO_2, wt.%	13.02	22.88	36.12	24	12.86	9.72	6.44	0.90
TiO_2	2.1	0.38	0.49	2.61	0.16	0.65	0.51	0.02
Al_2O_3	4.57	8.71	11.96	7.66	3.38	3.15	2.00	0.03
Fe_2O_3	0.01	0.17	1.02	1.2	0.70	0.05	n/d	0.2
FeO	7.00	2.00	3.00	5.6	4.50	5.8	6.50	1.30
MnO	0.31	0.25	0.42	0.25	0.36	0.49	0.32	0.28
MgO	2.93	1.54	1.3	4.6	1.23	0.83	0,65	0.55
CaO	41.26	33.36	21.00	25.5	49.00	45	48.66	54.66
Na_2O	0.90	2.50	5.20	1.5	2.20	1	0.50	0.4
K_2O	3.36	4.32	4.90	5.01	1.69	1.6	1.48	0.4
P_2O_5	2.45	0.79	0.42	0.03	1.21	2.07	2.37	1.22
S	n/d	n/d	0.80	0.2	1.31	0.82	1.24	n/d
LoI	19.8	19.4	12.7	20.6	23.1	27.85	28.5	38.3
Σ	97.71	96.30	100.25	98.76	101.70	99.03	99.17	98.26
Li, ppm	10	2.8	13	16	8	8	9	12
Rb	120	52	14	152	64	38	29	17
Sr	3953	9247	4051	3946	11,527	9114	21,982	16,498

End of Table 2

Mineral	Sample (sample N)							
	LPo1 (1)	354 (2)	D11-3 (3)	3-2 (4)	LPo2 (5)	Po-6 (6)	331 (7)	V348 (8)
Ba	3405	3054	380	1901	793	1060	282	542
V	239	61	56	212	108	76	134	13
Cr	53	25	7	85	14	16	5	11
Co	20	4.3	6	19	13	16	10	7
Ni	16	11	5	34	22	12	2.69	33
Cu	21	15	8	11	25	20	8	15
Zn	174	32	59	161	36	92	85	13
Y	61	98	47	42	88	100	73	138
Nb	123	57	660	153	1598	352	98	872
Ta	11	17	34	11	7	4	0.07	3.25
Zr	21	109	57	5	32	25	7	4.7
Hf	0.83	1.19	1.20	0.2	1.03	1	0.22	0.26
Pb	4.2	4.89	7	4	34	18	12	60
Th	1.94	3.07	19	0.9	19	12	14	2.81
U	0.4	1.01	32	3	27	11	n/d	5
La	191	370	373	147	388	356	926	849
Ce	394	641	618	287	731	740	1513	1176
Pr	56	70	66	36	71	96	121	141
Hd	211	221	198	130	239	356	385	433
Sm	31	31	22	19	41	53	58	50
Eu	9.57	8.95	5.84	6	11.7	15	16	12
Gd	29	25	14	14	39	41	43	43
Tb	2.70	3.04	1.81	1.8	4.03	4.8	6.0	4.93
Dy	14	15	10.7	10	23	26	31	26
Ho	2.48	3.10	2.13	1.9	4.33	4.8	5.82	5.85
Er	5.95	7.97	6.25	5.3	11.9	13	16	16
Tm	0.72	1.08	0.94	0.7	1.67	1.7	2.10	2.34
Yb	4.11	6.66	6.21	4.6	10.9	10	4	15
Lu	0.56	0.97	0.95	0.7	1.63	1.5	2.21	2.39
ΣREE + Y	1013	1504	1373	706	1666	1818	3212	2918
Sr/Ba	1.2	3.0	11	2.1	15	9	78	30
Nb/Ta	11	34	19	14	216	88	980	273
Zr/Hf	26	91	48	25	32	25	35	18
(La/Yb)n	31	37	40	22	24	24	45	38
Y/Ho	25	32	22	22	20	21	13	24
Eu/Eu*	0.96	0.96	0.95	1.08	0.89	0.95	0.94	0.77

Note. 1-4 – silicocarbonatites (sövites I): 1, 4 – Potanino deposit (CAB); 2 – root part of the Vishnevogorsky massif; 3 – apical part of the Vishnevogorsky massif; 5-8 – calciocarbonatites (sövites II): 5, 6 – Potanino deposit (CAB); 7, 8 – apical part of the Vishnevogorsky massif; n/d – not defined.

Table 3

Representative chemical compositions of the Buldym complex rocks

Mineral	Sample (sample N)								
	43332 (1)	505-27 (2)	15-22 (3)	T-1b (4)	K97-8 (5)	3296 (6)	43915 (7)	1-54 (8)	10-21 (9)
SiO_2, wt.%	41.39	37.71	40.40	7.40	3.08	3.51	3.61	0.72	30.50
TiO_2	0.02	0.02	0.04	0.07	0.03	0.02	0.02	0.18	0.11
Al_2O_3	0.73	0.76	1.24	1.40	0.56	0.74	0.73	0.02	1.29
Fe_2O_3	4.19	2.56	2.50	0.79	0.29	0.33	0.34	0.34	1.96
FeO	3.70	6.00	5.55	2.10	1.10	1.60	1.60	3.00	1.00
MnO	0.14	0.19	0.15	1.10	0.27	1.20	1.20	1.40	0.21
MgO	36.81	42.89	42.20	7.27	6.2	5.12	6.00	17.68	25.5
CaO	1.41	0.15	1.01	44.00	50.33	48.01	48.00	33.22	17.91
Na_2O	0.20	0.4	0.60	0.60	0.40	0.20	0.20	0.15	0.70
K_2O	0.02	0.12	0.40	1.09	0.54	0.68	0.68	0.01	0.01

355

End of Table 3

Mineral	Sample (sample N)								
	43332 (1)	505-27 (2)	15-22 (3)	T-1б (4)	K97-8 (5)	3296 (6)	43915 (7)	1-54 (8)	10-21 (9)
P_2O_5	0.01	0.01	0.02	0.01	0.03	0.01	0.01	0.18	1.35
LOI	12.2	7.2	4.6	34.5	38.45	38.4	38	43.2	17.8
Σ	100.82	98.02	98.71	100.33	101.27	99.82	99.50	100.1	98.34
Li, ppm	13	8	14	18	16	50	12	0.09	3.5
Rb	2.27	3.8	18	52	42	170	44	0.4	0.12
Sr	309	26	56	9547	6336	5600	10,279	6611	3796
Ba	28	24	42	484	198	140	224	233	302
Sc	5.2	6.0	8.2	5.8	0.57	2.0	2	1.15	1.78
V	22	19	29	67	1.18	20	15	8	51
Cr	1019	1451	911	138	23	50	107	23	35
Co	83	121	112	7	3.6	12	5	16	7
Ni	1519	1570	2363	13	39	190	10	13	30
Cu	19	26	18	24	32	3.8	24	20	24
Zn	39	50	52	88	14	110	49	47	8
Y	2.8	1.94	8	62	523	50	69	93	74
Nb	0.73	5.6	12	930	8	5800	20	88	15
Ta	0.07	0.33	0.04	1.24	0.27	7	0.02	0.08	0.14
Zr	11	1.69	5.0	42	0.64	4.0	2	24	37
Hf	0.28	0.05	0.12	0.51	0.40	–	0.1	0.43	0.46
Mo	0.50	0.58	0.07	0.62	0.07	0.90	0.6	1.20	0.00
Pb	2.34	0.10	2.84	23	38	11	14	23	59
Th	0.87	0.08	0.77	22	0.38	21	3	681	1418
U	0.12	0.02	0.03	n/d	0.04	9	n/d	n/d	n/d
La	6.01	1.12	5.78	577	1003	260	598	2285	19
Ce	9.21	2.82	12.6	1022	1822	400	1056	4092	25
Pr	0.79	0.37	1.51	58	168	40	59	180	913
Hd	2.76	1.58	6.11	180	550	130	202	543	2273
Sm	0.49	0.37	1.33	38	100	18	41	70	168
Eu	0.11	0.11	0.40	10	26	5.0	11	34	29
Gd	0.41	0.36	1.21	28	110	16	32	65	87
Tb	0.07	0.06	0.20	4.3	13	1.60	5	10	11
Dy	0.46	0.35	1.35	23	86	9	25	60	46
Ho	0.10	0.07	0.29	5.0	20	1.90	5.5	11	6.6
Er	0.28	0.22	0.81	14	65	6	16	23	12
Tm	0.05	0.03	0.13	2.20	10	0.90	2.4	3.0	1.31
Yb	0.33	0.25	0.91	15	71	6.0	17	16	6.2
Lu	0.05	0.04	0.13	2.37	10	1.10	2.6	2.04	0.77
ΣREE + Y	24	9.69	41	2043	4576	946	2141	7487	48,087
Sr/Ba	11	1.1	1.3	20	32	40	46	28	13
Nb/Ta	10	17	300	750	30	829	1000	1100	107
Zr/Hf	39	34	42	82	2	n/d	20	56	80
(La/Yb)n	12	3	4	26	10	29	24	96	2064
Y/Ho	28	28	28	12	26	26	13	8	11
Eu/Eu*	0.73	0.91	0.95	0.90	0.75	0.88	0.90	1.52	0.66

Note. 1-3 – ultramafic rocks: 1 – metaperidotite, 2 – metadunite, 3 – amphibole-phlogopite olivinite; 4-9 – carbonatites: 4-7 – dolomite-calcite carbonatites (sövites III); 8-9 – dolomite carbonatites (beforsites IV); (–) – below detection limit.

Ilmeno-Vishnevogorsky miaskite-carbonatite complex. According to the classification [32], most of the IVC rocks are represented by miaskites (leucocratic varieties of biotite-nepheline monzosyenites with oligoclase and orthoclase–perthite). The average content of orthoclase-perthite in miaskites is 50, oligoclase is 12, nepheline is 30-35 (in the Ilmenogorsky massif) and 28 % (in the Vishnevogorsky massif). Miaskites of the Vishnevogorsky massif contain 5-10 % of calcite.

Miaskites of the IVC are represented by plumasite (Al/(Na + K) mol. – 1.02-1.23, Al/(Na + K + 1/2Ca) mol. – 1.0-1.20), meta-aluminous varieties (Al /(Na + K + 1/2Ca) mol. – 0.83-0.98), containing 17.55-27.37 wt.% Al_2O_3 and alkalis 11.46-17.62 wt.% $K_2O + Na_2O$. The agpaitic coefficient (K_{agp}) in

miaskites usually varies from 0.82 to 0.98 and reaches agpaitic compositions (1.06) in antiperthite miaskites of the CAB (see Table 1) and taxitic varieties of miaskites of the Vishnevogorsky massif [14]. The compositions of the CAB miaskites are significantly different in the ratio of alkalis from the miaskites of the Vishnevogorsky and Ilmenogorsky massifs: the CAB miaskites are characterized by the Na-profile of alkalinity (K/Na mol. = 0.2-0.49); miaskites of the Vishnevogorsky and Ilmenogorsky plutons have K-Na type of alkalinity (K/Na mol. = 0.52-0.99) (Table 1) [14].

IVC miaskites show high content of high field strength elements (HFSE), ppm: Nb 45-200; Ta 2-20; Zr 40-150; Ti 4000-12,400; V 70-200. They are enriched in large-ion lithophile elements (LILE), ppm: Ba 1600-5600; Sr 1400-2500; Rb 34-114; Li 2-30, and REE 53-350. Miaskite-pegmatites are depleted in Sr (400 ppm), Ba (70 ppm), and REE (3.3 ppm) relative to intrusive varieties of miaskites, while the HFSE content: Nb (120 ppm), Ta (2 ppm), Zr (42 ppm) – is also high in them (Table 1).

Variations of petrogenic elements in the IVC carbonatites CaO (21.0-54.7 %) and low contents of FeO (1.32-7.0 %) and MgO (0.5-4.6 %) correspond to the compositions of calciocarbonatites (sövites) [31]. Sövites I differ from sövites II by increased contents of MgO (1.3-4.6 %), Al_2O_3 (4.57-11.96 %), SiO_2 (13-36.12 %).

Both varieties of the IVC carbonatites are enriched in HFSE and LILE, ppm: high contents of Nb to 1600, Zr to 110, V to 240; Sr 4000-22,000, Ba 300-3400, ∑REE 1000-3200 are close to the world average compositions of calciocarbonatites (Fig.1, *a, b*) [31]. Enrichment of carbonatites in niobium is largely associated with pyrochlore group minerals (uranium pyrochlore in silicocarbonatites; several generations of fluorocalciopyrochlore in sövites I and II).

Sövites I have high concentrations of Sr (3950-9250 ppm), Ba (380-3400 ppm), REE (700-1500 ppm) (but lower than in sövites II) and Eu/Eu* ratio (0.95-1.08), Sr/Ba (to 11), which is typical of high-temperature deep carbonatite facies (Table 2). Low ratios of Nb/Ta (< 35) and La/Yb$_n$ (< 40), high Eu/Eu* (about 1) in early carbonatites correspond to the initial stage of differentiation of carbonatite magmas [7]. Sövites II have the maximum contents of Sr (9110-21,980 ppm) and REE (1660-3210 ppm), high ratios of Nb/Ta (90-980) and Sr/Ba (to 78). There is a decrease to 0.77 Eu/Eu*, to 18 Zr/Hf, to 13 Y/Ho, which is typical of fluid-hydrothermal carbonate systems and late members of carbonatite series.

One of the probable mechanisms of the magmatic process of miaskite- and carbonatite formation in the IVC is the achievement by derivatives of the carbonatized miaskite melt of the so-called miscibility gap with subsequent stratification into leucocratic and melanocratic silicate and carbonate liquids, which is confirmed by the geochemistry of rare elements and the results of modeling magmatic processes [7]. Similar Sr-Nd isotopic compositions of carbonatites and miaskites also confirm the common source of their matter and the possible separation of carbonatite liquids from miaskite magmas [7].

According to thermobarometric data, IVC carbonatites are represented by high-temperature varieties of calciocarbonatites: silicocarbonatites (sövites I) with uranpyrochlore mineralization formed at temperatures of 830-650 (according to Ti-geothermometry in zircons [24]) and 730-770 °C (apatite-biotite geothermometer); sövites II with pyrochlore in paragenesis with apatite, calcite, biotite, ilmenite, pyrrhotite, and pyrite – at temperatures of 650-580 (Ti geothermometer in zircons [24]) and 590-490 °C (biotite-pyroxene and amphibole-pyroxene geothermometers [33]). Geothermobarometry of the IVC miaskite-pegmatites showed a close temperature range T = 800-650 °C and moderate pressures P = 3.5-2.5 kbar [33, 34].

In contrast to the intraplate carbonatite UACC complexes, the IVC does not contain late low-temperature ferrocarbonatite facies with Sr-Ba-REE mineralization. IVC carbonatites contain only accessory mineralization of HFSE (Nb, Zr, Ti), represented by pyrochlore, zircon, ilmenite, titanite, and ilmenorutile, while LILE minerals (Sr, REE, Ba) are very rare or absent in them. REE-Sr-Ba mineralization in IVC is more common in fenite aureoles in late feldspar, calcite, and quartz-arfvedsonite veinlets [35].

Buldym ultramafic carbonatite complex. The compositions of the Buldym complex carbonatites show wide variations in CaO (17.9-50.3 %) and MgO (5.1-25.5 %): the compositions of calcite-dolomitic carbonatites (sövites III) correspond to calciocarbonatites, and that of dolomitic carbonatites (beforsites IV), to magnesiocarbonatites [31].

Sövites III of the Buldym massif have close Sr and higher Nb (to 5800 ppm), as well as REE, Mn contents, increased HREE content and, accordingly, the minimum (La/Yb)*n* ratio (10-29) (Table 3) in comparison with the IVC carbonatites. They are close to the world average compositions of calciocarbonatite (Fig.1). The Nb content in them, like in the IVC carbonatites, is controlled by pyrochlore mineralization.

Beforsites of the Buldym massif are close to the world average compositions of magnesiocarbonatites [31] (Fig.1, *c, d*). They are noted for extremely high contents of REE (to 48,000 ppm) and Th (to 1400 ppm), which are concentrated in the form of monazite and aeschynite. Beforsites have low concentrations of Sr (3800-6600 ppm), Ba (230-300 ppm), and Nb (15-90 ppm) with maximum values and variations to 1100 Nb/Ta, 80 Zr/Hf and minimum 8-11 Y/Ho ratios, which is typical of the low-temperature members of the carbonatite series. The Eu/Eu* value also varies and reaches a minimum value of 0.65, which is typical of late hydrothermal stages of carbonatite formation [7].

According to dolomite-calcite thermobarometry, Buldym calciocarbonatites formed at temperatures of 575-410 °C and pressures of 1.6-0.9 kbar, and magnesiocarbonatites formed at lower temperatures and pressures, 315-230 °C and 0.9-0.36 kbar, respectively [29, 33]. Thus, in the Buldym complex, along with high-temperature varieties, calciocarbonatites with pyrochlore, there are also medium-temperature varieties of magnesiocarbonatites with REE- and Nb-mineralization (monazite-Ce, nioboaeschynite-Ce, magnesiocolumbite, less often chevkinite, fergusonite, orthite, fersmite). In contrast to the intraplate UACC, in the Buldym complex, as well as in the IVC, there are no low-temperature ferrocarbonatite facies with Sr-Ba-REE mineralization.

Rare metal (Nb-REE) ore mineralization. Ore concentrations of Nb in the IVC are associated with carbonatites and pegmatites and controlled by the distribution of minerals of the pyrochlore group. Accessory Nb-REE-bearing minerals, such as aeschinite-(Ce), aeschinite-(Y), columbite, chevkinite-(Ce), and fersmite, occur in syenite-pegmatites and late quartz-aegirine-arfvedsonite veins of fenite aureoles, but do not form ore concentrations [14].

In the Buldym complex, Nb deposits are linked with carbonatites and associated alkaline metasomatic rocks. The main ore mineral is pyrochlore, and minerals of the columbite and aeschynite groups are also present in significant quantities. In contrast to the IVC, carbonatites and metasomatic rocks of the Buldym complex contain widely developed ore Nb-REE- and REE-mineralization. The main REE mineral is monazite [14]. There are aeschynite-(Ce), orthite-(Ce), fergusonite-(Ce), chevkinite-(Ce), allanite; polyakovite-(Ce), bastnaesite-(Ce), synchisite-(Ce), parisite-(Ce), davidite-(Ce) are rarer [30].

The author's collections of pyrochlore from various deposits of the IVC and Buldym complex, as well as the collections of the deposit discoverer V.Ya.Levin were studied. The chemical composition of ore Nb-minerals of the pyrochlore group from the main types of the IVC and Buldym complex rocks was studied: samples of pyrochlores from miaskite-pegmatites (Uvildy ore occurrence, CAB); sövites I (Potanino deposit, CAB); sövites II (Vishnegorskoye and Potanino deposits) were studied in the IVC. In the Buldym complex, pyrochlores from sövites III (Buldymskoye deposit) were investigated.

IVC pyrochlores forms in pegmatoid varieties of miaskites, miaskite- and syenite-pegmatites, melanocratic glimmerite-like carbonate-silicate rocks, fenites, phlogopite-richterite metasomatic rocks and, in the most significant quantities, carbonatites. In pegmatoid varieties of miaskites, pyrochlore is present as disseminated black (uranium pyrochlore), dark brown, less often light brown grains and crystals of octahedral habit to 0.5 cm in size, in miaskite-pegmatites, to 10 cm. It also occurs as inclusions 100-200 µm in size in grains of nepheline, feldspars, and zircon (Fig.2, *a*). Many pyrochlore crystals of miaskite-pegmatites contain oriented plates of ilmenite − intergrowth
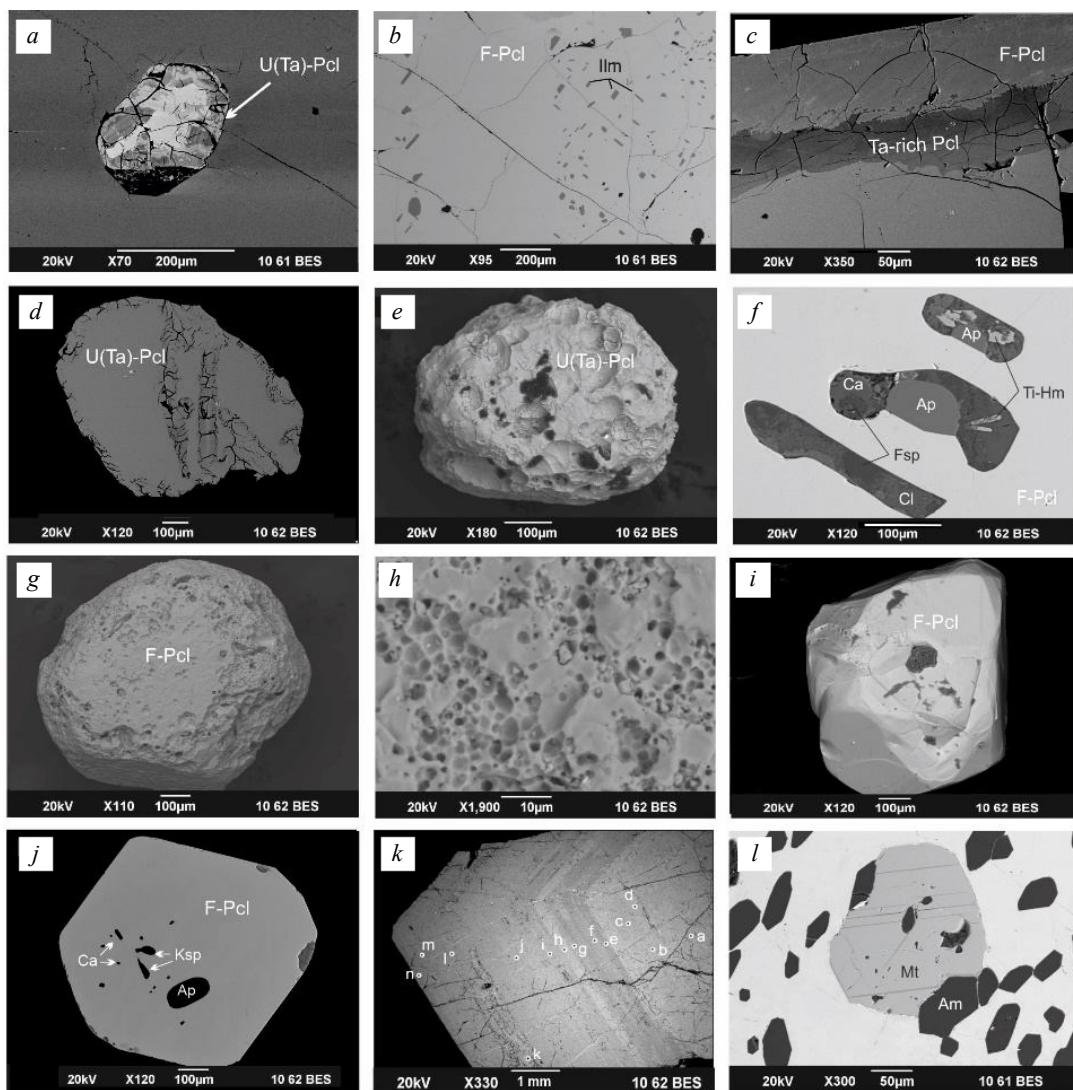
Fig.2. Morphology and features of the internal structure of pyrochlore crystals from the IVC and Buldym complex of the Urals: *a-c* – pyrochlores of miaskite-pegmatites: *a* – U-(Ta)-pyrochlore grain in zircon (solar nepheline mine, CAB); *b* – pyrochlore with oriented ilmenite plates (vein N 5, Karavai town, Vishnevogorsky massif); *c* – Ta-enriched zone of alteration in a pyrochlore crystal (vein N 5, Karavai town, Vishnevogorsky massif); *d-f* – pyrochlores of silicocarbonatites (sövites I): *d* – grain of U-(Ta)-pyrochlore hydrated along the periphery and internal cracks (Uvildy ore occurrence, CAB); *e* – U-(Ta)-pyrochlore grain with spherical caverns (Potanino deposit, CAB); *e* – multiphase inclusions in pyrochlore grain (Potanino deposit, CAB); *g-m* – sövite II pyrochlores: *g, h* – pyrochlore crystal containing bubbles in the marginal part (Potanino deposit, CAB); *i* – cuboctahedral pyrochlore crystals (Vishnevogorskoye deposit); *j* – pyrochlore crystal with inclusions of apatite, calcite, feldspar (Vishnevogorskoye deposit); *k* – growth zoning in a pyrochlore crystal (Vishnevogorskoye deposit); *m* – pyrochlore crystals with inclusions of amphibole and magnetite from phlogopite-richterite metasomatic rocks (Buldymskoye deposit)

U(Ta)-Pcl – uranium pyrochlore; F-Pcl – fluorcalcipyrochlore; Am – amphibole; Mt – magnetite; Ti-Hm – titanium-hematite; Ilm – ilmenite; Ca – calcite; Ap – apatite; Cl – chlorite

structures (Fig.2, *b*). Sometimes zoning is observed [36], and in the edge parts of crystals there are zones of hydrothermal alterations enriched in Ta (Fig.2, *c*).

In silicocarbonatites (sövites I) and glimmerite-like rocks of the CAB, pyrochlore is represented by a U-(Ta)-rich variety (uranium pyrochlore) and occurs in the form of small (0.05-1 mm) crystals and round black grains, often with a cavernous surface (Fig.2, *d, e*). Sövites I contain dark brown pyrochlore crystals with multiphase inclusions (apatite, calcite, potassium feldspar, chlorite,

titanhematite) (Fig.2, *f*). In both varieties of the CAB pyrochlores, both in the inner and outer parts of the crystals, hollow spheres less than 10 μm in size are found (Fig.2, *g, h*). They may be associated with a high fluid saturation of the melt and degassing of carbonatite magmas.

In carbonatites (sövites II) of the Vishnevogorsky massif, pyrochlores are found in the form of octahedral and cuboctahedral crystals (Fig.2, *i-l*) 0.05-1.5 cm in size, red-brown, bright red, yellow and orange. They are characterized by syngenetic inclusions of apatite, calcite, feldspar (Fig.2, *l*). Sometimes there is visible growth zoning in pyrochlore crystals (Fig.2, *k*) [36]. There are crystals of a complex structure, with relic dark cores surrounded by a border of red pyrochlore.

In dolomite-calcite carbonatites (sövites III) of the Buldym complex, pyrochlore forms large brownish-red crystals and grains (0.5-10 cm in size). In phlogopite-richterite metasomatic rocks associated with carbonatites, there is a small dissemination of yellowish-brown pyrochlore with numerous inclusions of amphibole (fluorrichterite) (Fig.2, *l*). Uranium pyrochlore (rounded black grains 0.1-0.5 cm) and dark brown REE-Th-pyrochlore intergrown with aeschynite were found in glimmerites.

According to the latest nomenclature of the pyrochlore group [37], the compositions of pyrochlores from the IVC and the Buldym carbonatite complex of the Urals are represented by U-(Ta)-rich oxy- and hydroxylcalcipyrochlores (or uranium pyrochlores [38]), fluorocalciopyrochlores (Ta-, REE-Sr-containing varieties), as well as hydroxyl- and hydropyrochlores formed during the secondary alterations of early generation pyrochlores (Table 4).

Table 4

Representative compositions of the pyrochlore group minerals in carbonatite complexes of the Urals, wt.%

Mineral	Sample (sample N)								
	Soln-1 (1)	3795_34 (2)	Kv-5-2 (3)	43-62 (4)	140-39 (5)	3296 (6)	Dol-7 (7)	84-2kr (8)	331-1-2k (9)
	Pcl I		Pcl II		Pcl III		Pcl IV		Pcl V
Nb_2O_5	40.98	45.31	59.85	63.04	65.60	66.64	67.14	61.46	60.23
Ta_2O_5	3.96	5.01	2.55	2.76	0.09	–	–	–	0.27
SiO_2	–	–	0.01	–	–	0.02	–	–	4.99
TiO_2	12.32	10.34	4.70	4.71	4.98	3.29	3.52	6.07	5.06
UO_2	23.50	17.27	4.66	0.15	0.09	0.17	0.09	0.77	0.57
ThO_2	0.51	0.93	0.27	2.15	0.26	0.54	0.41	0.45	0.78
Fe_2O_3	0.11	0.15	–	0.05	0.02	0.13	–	–	1.59
Y_2O_3	–	–	0.05	–	–	0.03	–	–	0.04
La_2O_3	0.00	0.09	0.06	–	0.5	0.08	0.65	1.06	1.49
Ce_2O_3	0.00	0.77	0.06	0.72	1.05	0.24	1.33	3.46	4.52
Nd_2O_3	0.10	0.3	0.19	0.17	0.22	0.14	0.23	1.07	n/d
MnO	0.05	0.02	–	–	0.02	–	–	–	0.74
CaO	12.03	12.2	15.19	15.98	16.44	16.27	13.74	13.46	6.69
BaO	0.02	–	–	–	–	–	–	–	1.58
SrO	–	–	0.55	0.49	0.51	0.67	2.15	1.71	4.40
PbO	1.01	0.80	0.06	–	0.19	–	но	–	0.46
Na_2O	5.12	5.52	7.01	6.49	7.07	7.42	7.37	6.89	0.35
F	0.95	1.59	4.01	4.49	4.60	4.39	4.68	4.42	0.50
Total	100.66	100.39	99.20	101.19	101.64	100.02	101.31	100.82	94.26
$O = F_2$	0.40	0.67	1.69	1.89	1.94	2.14	1.97	1.86	0.21
Sum	100.26	99.72	97.51	99.30	99.71	97.87	99.34	98.96	94.05
Nb, formula units	1.280	1.376	1.729	1.736	1.774	1.842	1.840	1.718	1.460
Ta	0.074	0.093	0.044	0.046	0.001	–	–	–	0.004
Ti	0.640	0.523	0.226	0.216	0.224	0.151	0.160	0.282	0.204
Fe^{3+}	0.006	0.008	–	0.002	0.001	0.006	–	–	0.064
Si	–	–	0.001	–	–	0.001	–	–	0.268
Sum B	2.000	2.000	2.000	2.000	2.000	2.000	2.000	2.000	2.000
Ca	0.890	0.878	1.004	1.043	1.053	1.065	0.892	0.894	0.384
Mn	0.003	0.001	–	–	0.001	0.001	–	–	0.034

End of Table 4

Mineral	Sample (sample N)								
	Soln-1 (1)	3795_34 (2)	Kv-5-2 (3)	43-62 (4)	140-39 (5)	3296 (6)	Dol-7 (7)	84-2kr (8)	331-1-2k (9)
	Pcl I		Pcl II		Pcl III		Pcl IV		Pcl V
Ba	0.001	–	–	–	–	–	–	–	0.033
Sr	–	–	0.020	0.017	0.018	0.024	0.076	0.061	0.137
Pb	0.019	0.014	0.001	–	0.003	–	n/d	–	0.007
Na	0.686	0.719	0.869	0.767	0.820	0.879	0.866	0.826	0.036
Y	–	–	0.002	–	–	0.001	0.000	–	0.001
LREE	0.002	0.028	0.007	0.020	0.039	0.010	0.049	0.126	0.118
U	0.361	0.258	0.066	0.002	0.001	0.002	0.001	0.011	0.007
Th	0.008	0.014	0.004	0.030	0.004	0.008	0.006	0.006	0.001
Sum A	1.970	1.914	2.010	1.879	1.938	1.989	1.890	1.922	0.767
A-deficiency	0.03	0.086	–0.010	0.121	0.062	0.011	0.110	0.078	1.233
F	0.208	0.338	0.810	0.865	0.870	0.849	0.897	0.865	0.085

Note. Pcl I – Pcl V – pyrochlore generations; 1-2 – uranium pyrochlore I (hydroxylcalcipyrochlore [37]): 1 – from miaskite-pegmatite (Uvildy ore occurrence, CAB); 2 – from sövite I (Potanino deposit, CAB); 3-4 – pyrochlore II (Ta-containing fluorocalcio-pyrochlore [37]): 3 – from miaskite-pegmatite (vein no. 5, Vishnevogorskoye deposit); 4 – from sövite I (Potanino deposit, CAB); 5-6 – pyrochlore III (fluorocalciopyrochlore [37]): 5 – from sövite II (ore zone 140, Vishnevogorskoye deposit); 6 – from sövite III (Buldymskoye deposit); 7-8 – pyrochlore IV (Sr-REE-containing fluorocalciopyrochlore [37]): 7 – from sövite II (ore zone 147, Vishnevogorskoye deposit); 8 – from sövite II (fenite aureole, Potanino deposit); (9) pyrochlore V (Sr-Ba-Si-REE-rich hydropyrochlore [37]) from sövite II (Vishnevogorskoye deposit). The formulas are calculated for two cations in the B-position. A-deficiency – the number of vacancies in the A-position.

U-(Ta)-hydroxylcalciopyrochlore (uranpyrochlore I [38]) with a high content of UO_2 (17-24 wt.%) and Ta_2O_5 (4-5 wt.%). It occurs in pegmatoid miaskites, miaskite-pegmatites, and silicocarbonatites (Potanino deposit, Uvildy ore occurrence); in the Buldym complex, in glimmerite-like rocks. Uranium pyrochlores in the IVC formed earlier than other types of pyrochlores, at the late magmatic stage of the evolution of alkaline carbonatite magmas [5, 14].

U-(Ta)-containing fluorocalciopyrochlore (II) with a lower UO_2 content (0.15-4.66 wt.%), rich in Ta_2O_5 (2.55-2.76 wt.%) and F (4.0-4.5 wt.%). It occurs in the most evolved types of miaskite-pegmatites (ore zones 147 and 140 of the Vishnevogorskoye deposit) and early high-temperature facies of silicocarbonatites (sövites I) at the Potanino deposit. It formed at the late magmatic (pegmatite and early carbonatite) stage of crystallization of alkaline carbonatite melts [5].

Fluorocalciopyrochlore (III) does not contain microimpurities (including Ta and U), with high F contents (4.4-4.6 wt.%). It is widespread in carbonatites (sövites II) of the Vishnevogorsky and Buldym massifs, as well as in richterite-phlogopite metasomatic rocks associated with carbonatites in the Buldym complex, which suggests the possibility of its formation from alkaline carbonate fluids with a high F content.

Sr-REE-containing fluorocalciopyrochlore (IV), enriched in SrO (1.7-2.15 wt.%) and $LREE_2O_3$ (2.2-5.6 wt.%), compared with early generations, with high F (4 .4-4.7 wt.%). It occurs in late carbonatites (sövites II) of the Vishnevogorsky massif and fenite aureoles. The formation of such pyrochlore varieties, as in other alkaline complexes [39], probably occurs at the final stages of evolution with the participation of fluorine-containing fluids.

The latest generations of pyrochlore, represented by hydroxylcalciopyrochlore and hydropyrochlore (V), enriched in Sr, Ba, Si, REE (sometimes Ta, U), formed in the IVC and Buldym complex as a result of alterations of primary pyrochlores [5]. Their formation may be associated with subsolidus and hydrothermal processes at the final stage of magmatic evolution, as in other carbonatite complexes, as well as with the processes of metasomatism and collisional metamorphism.

Discussion of the results. Linear carbonatite complexes of the Urals are representatives of deformed alkaline carbonatite complexes, which are called DARC (Deformed Alkaline Rocks with

Carbonatite) in the English-language literature [9]. Deformation textures (gneissocity, banding, boudinage, folding) are common for the IVC and Buldym carbonatite complex rocks. Preserved igneous structures of rocks, miaskite compositions corresponding to eutectic crystallization, distinct intrusive boundaries of massifs, the presence of vein bodies of miaskite-aplites and miaskite-pegmatites testify to the igneous origin of the IVC.

Intraplate rifting is the main tectonic setting where nepheline-bearing syenites and carbonatites are generated [9, 40, 41]. Deformed alkaline rock and carbonatite complexes (DARC) [40] are earlier rift-related alkaline complexes of intraplate settings that were later involved in the collision zone, deformed, and, in some cases, subjected to melting. For some DARC complexes, another generation mechanism was proposed, associated with collisional strike-slip tectonics and an intra-orogenic extension phase, which ends with a subsequent compression phase [10-12].

Figure 3, *a, b* shows a comparison of the concentrations of REE (normalized by chondrite) and trace elements (normalized by primitive mantle) in the studied alkaline rocks of the IVC with data published for alkaline complexes of intraplate settings, for nepheline-bearing syenites and carbonatites of the East African rift (Kasungu, Chipala, Bingo), Malawi [42], and the Karelian-Kola province (Khibiny, Lovozero) [43]. Trace element spider diagram show similarities between the IVC miaskites and East African Rift alkaline rocks, demonstrating enrichment in HFSE (Nb, Ta, Zr, Hf, Ti) as well as LILE (Ba, Sr, Rb) and REE (Fig.3, *b*). The IVC miaskites in spider diagrams show more pronounced maxima of Ba and Sr and some depletion in Nb, Ta, Zr, Hf, Ti and REE of the most evolved (agpaitic) varieties of rocks of the intraplate UACC complexes (Fig.3, *b*). Their compositions are close to those of the parent magmas of the carbonatite complexes of the Kola Province (Fig.3, *a, b*) [38, 39]. The composition of trace elements and trends in the evolution of the IVC miaskites are similar to the early phases of nepheline syenites in the UACC complexes of intraplate settings [44].

The REE spectra of the IVC nepheline syenites and rift-related intraplate complexes have a similar REE patterns with highly enriched LREEs and almost flat HREEs relative to chondrite (Fig.3, *a*). However, the IVC miaskites have lower REE than nepheline syenites of the East African Rift and the most evolved (agpaitic) rock varieties of the Kola Province (Fig.3, *a*). The $(La/Yb)n$ values of 23-89 for the IVC miaskites are similar to nepheline syenites of the Kola Province and somewhat higher than for their equivalents (12-35) from the East African Rift. Differences in REE in these groups of nepheline syenites may be due to differences in source, degree of melting, and depth of magma generation. The high $(La/Yb)n$ values of the IVC miaskites indicate a metasomatized mantle source, while the low HREE and high $(Gd/Yb)n = 2$-2.8 (except for the miaskite-pegmatites) suggest the generation of the IVC magmas near the garnet stability field under conditions of deep facies of garnet peridotites [45].

Figure 3, *c, d* shows the results of a comparison of the REE and rare-metal composition in miaskites of the IVC and nepheline syenites of deformed alkaline complexes (DARC) of the Indian Fold Belt (Santori) [41] and the Central Andes (Argentina) [46], which are deformed rift-related complexes involved in the collision zone [47]. IVC miaskites are compared with DARC syenites of the Himalayan collisional zone (Maoniuping, Dalukao, Lizuang, South China), generated and deformed at the collisional stage of orogen development [48].

Deformed rift-related complexes (DARC) and the IVC show similar REE distribution with LREE enriched and close $(La/Yb)n$ ratios (50.13-109.51 in Indian nepheline syenites; 22.6-89.43 in the IVC miaskites) (Fig.3, *c*), as well as almost identical spider diagrams, illustrating close contents of HFSE and LILE in these complexes (Fig.3, *d*). This may indicate similar conditions for magma generation in the complexes (source composition, degree of melting, and depth of magma generation) [42]. While the synorogenic syenites of the Himalayan collision zone differ significantly from the IVC miaskites and nepheline syenites of the deformed rift-related complexes in high contents and significant variations in REE and $(La/Yb)n$ (3-248), depletion of HFSE (Nb, Ta, Ti), and enrichment of LILE (Ba, Sr, Rb), as well as Pb, Th, U (Fig.3, *c, d*).
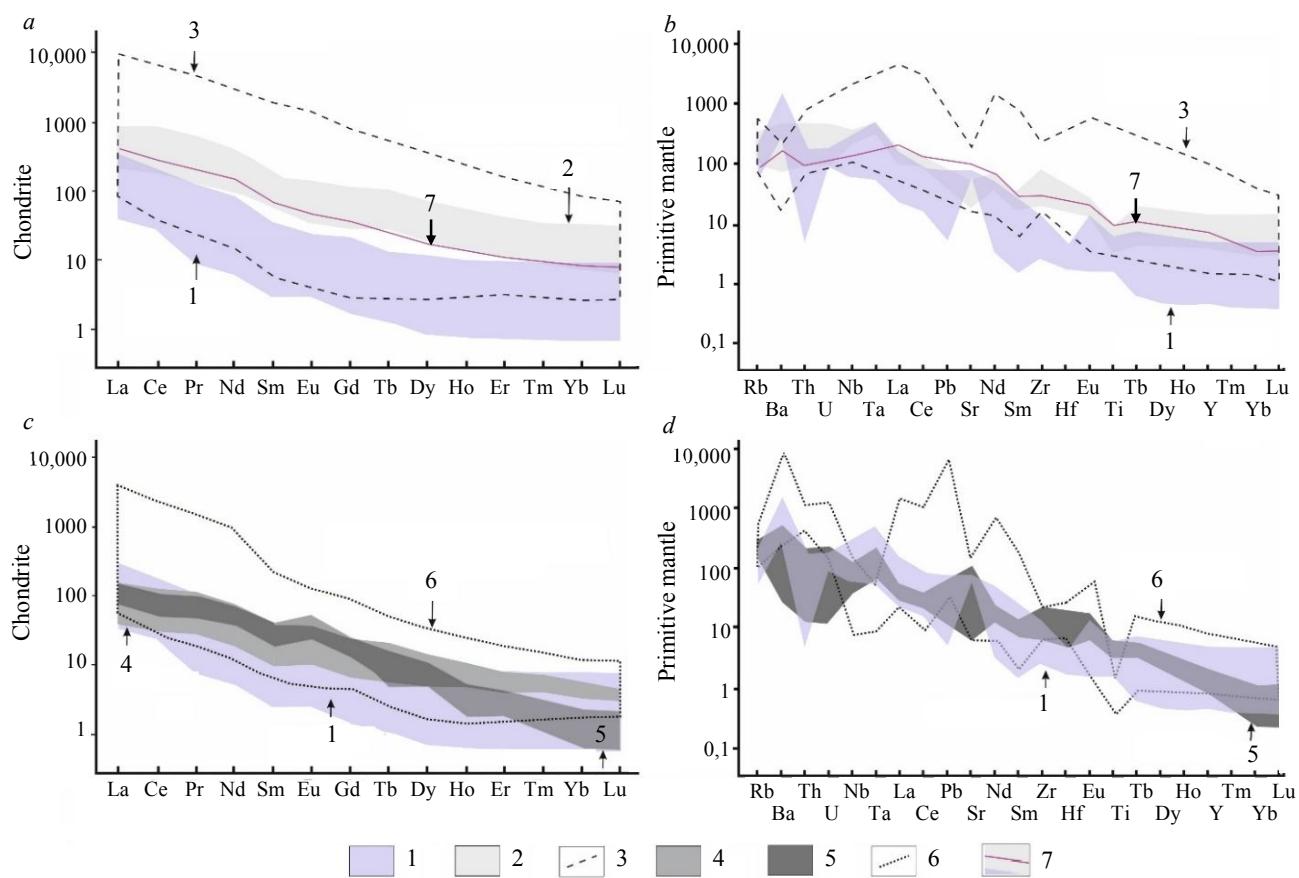
Fig.3. Comparative study of chondrite-normalized REE contents and spider diagrams of nepheline syenites from the IVC
of the South Urals, their comparison with rift-related alkaline rocks of intraplate settings, the East African Rift (Bingo, Chipala,
Kasungu) [42] and the Kola Province (Khibiny, Lovozero) [50, 51] (*a, b*); with deformed carbonatite complexes (DARC) of
intraplate rift origin (Pampeano, Central Andes [46]; Santouri, India [47]) and synorogenic origin (Maniuping, Dalukao, Dizuang,
Himalayas [48]) (*c, d*)

1 – miaskites of the IVC, South Urals, Russia; 2, 3 – intraplate rifto-related complexes of ultramafic alkaline rocks and carbonates (UACC):
2 – Bingo, Chipala, Kasungu, East African Rift (Eby et al., 1998; Wooley et al., 1995); 3 – Khibiny, Lovozero, Kola Province (Downes et al., 2005);
4-6 – deformed complexes of alkaline rocks and carbonatites (DARC) of various tectonic settings: 4 – DARC rift-related, Pampeano, Central Andes,
Argentina (Casquet et al., 2008); 5 – DARC rift-related, Santuri, Great Indian Belt, India (Das et al., 2018); 6 – DARC orogenic, Maoniuping,
Dalukao, Lizuang, Himalayas, China (Hou et al., 2006); 7 – parental melt of the Kola UACC province (Arzamastsev and Mitrofanov, 2009)

Fig.4, *a, b* shows the comparison of rare and rare-earth elements in carbonatites from the IVC and Buldym complex of the South Urals with carbonatites from rift-related complexes of intraplate settings (Belaya Zima, East Sayan province [49]; Kovdor and Khibiny, Kola province [50]). Fig.4, *c, d* compares them with carbonatites of deformed carbonatite complexes (DARC): the Pampeano rift-related deformed complex, Central Andes (Argentina) [46] and the DARC complexes of the Himalayan collision zone (Maoniuping, Dalukao, Lizuang, South China), generated during orogenesis [48]. For comparison, we used the compositions of early high-temperature varieties corresponding to calciocarbonatites [31]: sövites I and II in IVC; sövites III in the Buldym complex.

Calciocarbonatites of the IVC and Buldym complex are enriched in HFSE and LILE. Their content is comparable to the average composition of calciocarbonatites of the World (Fig.4, *a, b*) [31]. They are characterized by significant contents of HFSE elements, Nb, Ta, Ti, and, to a lesser extent, Zr, Hf, similar to the contents in the rift-related circular UACC complexes of the intraplate settings (Fig.4, *b*). Compared to the UACC complexes, calciocarbonatites of the Urals are enriched in Sr and REE, are characterized by flatter REE spectra relative to chondrite (Fig.4, *a, b*). Low ratios of Nb/Ta (< 35) and La/Yb (< 60), high Eu/Eu* (about unity) in silicocarbonatites indicate a lower degree of differentiation of the IVC carbonatite magmas.

Spider-diagrams of carbonatite complexes of the Urals and deformed rift-related carbonatite complexes of intraplate settings (Fig.4, *c, d*) illustrate a similar level of REE contents, with different (La/Yb)*n* ratios (50.13-109.51 in the deformed Pampeano carbonatites; 21.57-44.65 in the IVC carbonatites), and similar HFSE and LILE contents. Synorogenic calciocarbonatites of the Himalayan collision zone differ significantly from carbonatites of the Ural complexes by the high content of LILE (Ba, Sr), LREE (Th, Pb) and the strong depletion of HFSE (Nb, Ta, Zr, Hf, Ti) (Fig.4, *c, d*), as well as the absence of Nb mineralization [48].

Judging by the significant similarity of the geochemical features in the studied rocks of the Ural carbonatite complexes with other nepheline syenites and carbonatites of intraplate rift-related origin, including deformed rift-related complexes (DARC), we can assume that magmas of the Ural carbonatite complexes were intruded into the continental rift zone. The primitive character of the IVC nepheline-syenite and carbonatite magmas, in comparison with the rift-related UACC complexes, suggests their formation at the stage of transition from extensional tectonics to tangential compressional tectonics.

Petrochemical and geochemical features of the IVC miaskites and carbonatites (slight depletion of HFSE – Nb, Ta, Zr, Hf, Ti, enrichment of LILE, in particular K, Ba and Sr, in miaskites, Sr, REE
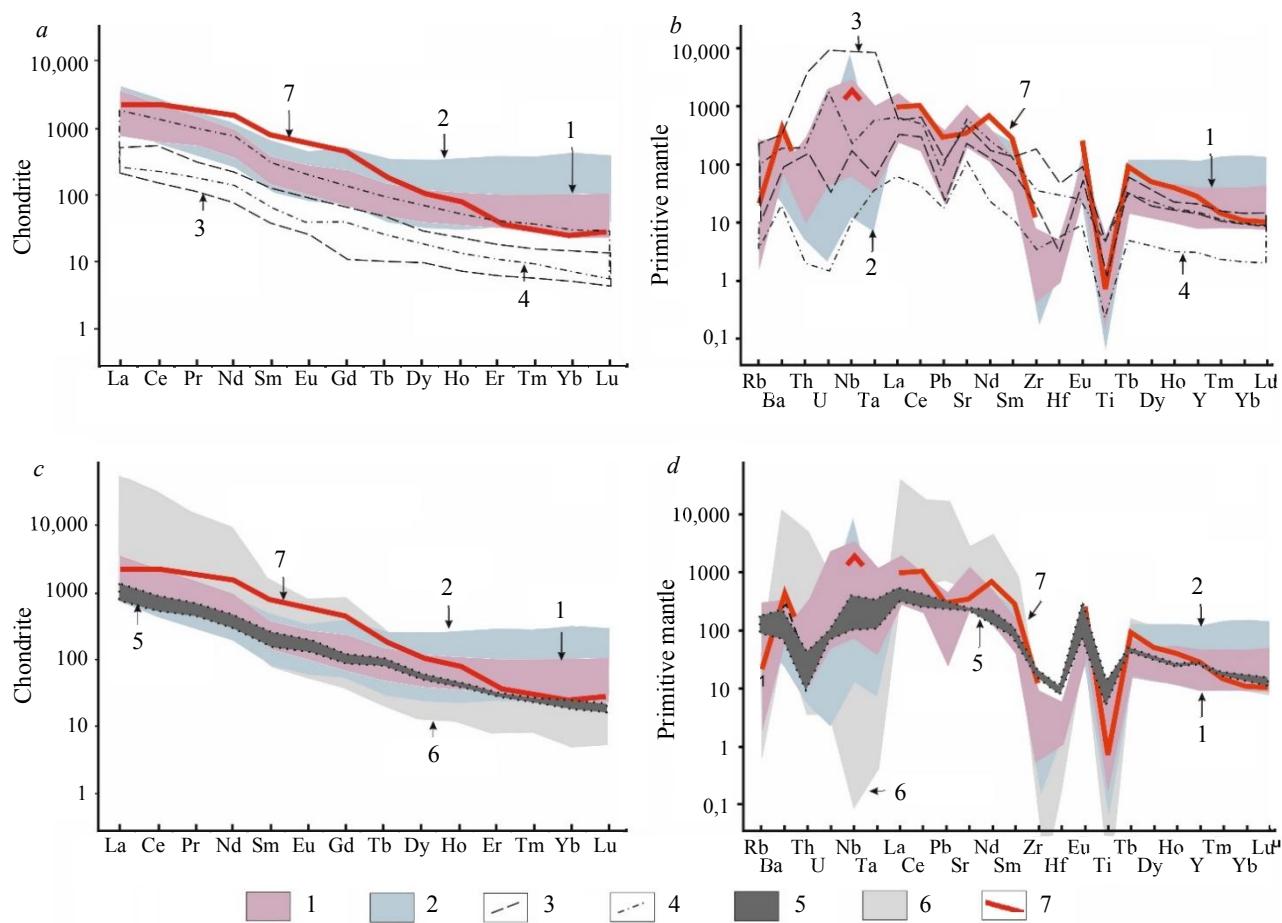
Fig.4. Chondrite-normalized REE contents and spider-diagrams of calciocarbonatites of the IVC and Buldym complex of the South Urals and their comparison: *a, b* – with rift-related calciocarbonatites of intraplate settings (Belaya Zima, East Sayan province [49]; Khibiny, Kovdor, Kola province) [50]; *c, d* – with deformed carbonatite complexes (DARC) of intraplate rift-related origin (Pampeano, Central Andes [40]) and synorogenic DARC complexes (Maniuping, Dalukao, Lizuang, Himalayas [48])

1 – calcicarbonatites (sövite I, II), IVC, South Ural, Russia; 2 – calciocarbonatites (sövite III), Buldym complex, South Urals, Russia; 3-4 – intraplate rift-related carbonatite complexes: 3 – Belaya Zima, East Sayan province (Khromova et al., 2020); 4 – Khibiny, Kovdor, Kola province (Downes et al., 2005); 5-6 – deformed carbonatite complexes (DARC) of various tectonic settings: 5 – rift-related DARC, Pampeano, Central Andes, Argentina (Casquet et al., 2008); 6 – orogenic DARC, Maniuping, Dalukao, Lizuang, Himalayas, China (Hou et al., 2006); 7 – intermediate composition of calciocarbonatite (Wooley and Kempe, 1989)

in carbonatites) relative to intraplate carbonatite complexes can be associated with their tectonic position near the craton margin, where carbonatite magmas depleted in Nb, Ta and enriched in Sr, Ba, and REE are generated [52]. Enrichment of the IVC miaskites and carbonatites in LILE-elements can be associated with the peculiarities of the evolution of fluid-saturated nepheline-syenite and carbonatite magmas and wide development in the IVC and Buldym complex, along with igneous varieties, of carbonatites formed from high-temperature fluid hydrothermal carbonate systems.

IVC carbonatites and miaskites significantly differ from the rocks of synorogenic carbonatite complexes, which are poor in Nb and Ta and lack Nb mineralization. Synorogenic carbonatite magmas, in contrast to the Ural carbonatite complexes, have a pronounced REE-Ba-Sr specialization and often produce commercially significant REE deposits (for example, Maoniuping, Dalukao, Mayaning-Dichang province, China [48]).

Comparison of carbonatite complexes of the Urals with carbonatite complexes of different geodynamic settings showed that the rift-collision model of DARC formation proposed by K.Burke and S.Khan [9, 40] is applicable for the IVC and Buldym complex of the South Urals. According to this model, alkaline-carbonatite magmas of the Ural complexes were intruded continental rift margins in the Paleozoic (O_3-S) [13, 20, 24]. Approximately at the same time, Paleozoic (O-S) mafic-ultramafic complexes developed during the opening of the Ural Ocean and island-arc volcanogenic-sedimentary complexes (O_3-D_3) [18] formed in the Urals, indicating a change in the tectonic regime and the transition from extensional tectonics to compression. Later on, continental margin rift-related carbonatite complexes were captured, deformed, and remelted in the suture zone after the closure of the Ural Ocean and the collision of the East European, Siberian, and Kazakhstan continents (~380-360 Ma – early collision, D_3; ~320-280 Ma – later collision, C_1-P_1 [18]). Deformation banding, cataclasis, and brecciation arose during the postmagmatic and metamorphic evolution of the IVC. Large-scale recrystallization of rocks and ores [20, 27], as well as pegmatite and syenite formation [53], are associated with the postorogenic stage of the IVC and Buldym complexes formation and postcollisional extension (~250 Ma).

The geodynamic model of the Ural carbonatite complexes formation is based on age data obtained using isotope dating methods. However, the interpretation of geochronological data as applied to deformed complexes of alkaline rocks and carbonatites (DARC) is often ambiguous [12] and requires preliminary detailed mineralogical studies, knowledge of the laws of mineral anatomy and ontogenesis, as well as solving the issues of petro- and ore genesis [54-56]. For the DARC carbonatite complexes, it is especially important to use the U-Pb geochronological data obtained from zircons correctly, since these complexes contain zircon generations of different ages (including inherited and newly formed) [12, 20]. The dating of carbonatite and ore formation processes should be carried out considering additional mineralogical and geochemical information [57-59].

Conclusion. IVC carbonatites are represented by high-temperature varieties of silico- and calico-carbonatites enriched in HFSE- and LILE-elements and contain ore pyrochlore mineralization. U-Ta-rich populations of uranium pyrochlores (I) and fluorocalciopyrochlores (II) crystallize in miaskite-pegmatites and silicocarbonatites at the early stages of the evolution of alkaline carbonatite magmas. Fluorcalciopyrochlores (III) and Sr-REE-rich pyrochlores (IV) of late populations form in late calciocarbonatites and fenites, probably with the participation of alkaline carbonate fluids. In the Buldym complex, along with medium-temperature varieties of calciocarbonatites, magnesiocarbonatites with ore REE-Nb mineralization (monazite, aeschinite, columbite, etc.) are widespread. In contrast to the carbonatite complexes of collisional origin, the IVC and Buldym complex do not contain late carbonatite facies with Sr-Ba-REE mineralization.

A comparative analysis of the geochemistry and petrochemistry of rocks from the carbonatite complexes of the Urals showed that the IVC miaskites and carbonatites are characterized by significant contents of HFSE (Nb, Ta, Zr, Hf, Ti) and LILE (Sr, Ba, Rb, Li), which are close to the contents in rift-related carbonatite complexes of intraplate settings (especially in the complexes of the Kola province and the East African Rift) and continental margin deformed carbonatite complexes (DARC)

of rift-related origin (Pampeano, Central Andes, Argentina; Santuri, India). The complexes of the Urals differ significantly from the synorogenic carbonatite complexes (in particular, from the complexes of the Himalayan collision zone), which, in comparison with the Urals, are enriched in LILE, Pb, Th, U and depleted in HFSE. REE deposits are associated with them, but there is no Nb mineralization.

The Ural complexes of alkaline rocks and carbonatites formed in marginal continental rifts in the Paleozoic ($\sim$440-420 Ma, O_3-S) during the Ural Ocean opening, at the stage of transition from extensional tectonics to compressional tectonics. They were later captured, deformed, and underwent partial melting in the suture zone as a result of collision of the East European, Siberian, and Kazakhstan continents ($\sim$320-280 Ma, C_1-P_1). Recrystallization of rocks and ores of carbonatite complexes, plastic and brittle deformations, as well as pegmatite and syenite formation are associated with the orogenic and postcollisional ($\sim$250-240 Ma) stages of development of the Ural folded region. Questions of the genesis and age of rare metal mineralization of the Ural carbonatite complexes and its relationship with various geodynamic settings are a priority for further research.

REFERENCES

1. Kogarko L.N., Kononova V.A., Orlova M.P., Wooley A.R. Alkaline Rocks and Carbonatites of the World. London: Former USSR, Chapman and Hall, 1995. Part 2, p. 226.

2. Frolov A.A., Belov S.V. Carbonatite deposits in Russia. Moscow: NIA-Priroda, 2003, p. 494 (in Russian).

3. Vladykin N.V., Pirajno F. Types of carbonatites: Geochemistry, genesis and mantle sources. *Lithos*. 2021. Vol. 386-387. N 105982. DOI: 10.1016/j.lithos.2021.105982

4. Vrublevskii V.V., Doroshkevich A.G. Isotope Systematics of Alkaline Rocks and Carbonatites in the Northern and Western Asia Folded Areas: A New Data Review. *Geosphere Research*. 2021. N 4, p. 6-26 (in Russian). DOI: 10.17223/25421379/21/1

5. Nedosekova I., Vladykin N., Udoratina O., Belyatsky B. Ore and Geochemical Specialization and Substance Sources of the Urals and Timan Carbonatite Complexes (Russia): Insights from Trace Element, Rb-Sr, and Sm-Nd Isotope Data. *Minerals*. 2021. Vol. 11. Iss. 7. N 711. DOI: 0.3390/min11070711

6. Castor S.B. The Mountain Pass rare-earth carbonatite and associated ultrapotassic rocks, California. *Canadian Mineralogist*. 2008. Vol. 46. N 4, p. 779-806. DOI: 10.3749/canmin.46.4.779

7. Nedosekova I.L., Belousova E.A., Sharygin V.V. et al. Origin and evolution of the Il'meny–Vishnevogorsky carbonatites (Urals, Russia): Insights from trace–elements compositions, Rb-Sr, Sm-Nd, U-Pb and Lu-Hf isotope data. *Mineralogy and Petrology*. 2013. Vol. 107, p. 101-123. DOI: 10.1007/s00710-012-0223-9

8. Vrublevskii V.V., Bukharova O.V., Nebera T.S., Sveshnikova V.L. Composition and origin of rare-metal (Nb-Ta, REE) and sulfide mineralization in magnesiocarbonatites from the Yenisei Ridge, Central Siberia. *Ore Geology Reviews*. 2019. Vol. 111. N 102949. DOI: 10.1016/j.oregeorev.2019.102949

9. Burke K., Ashwal L.D., Webb S.J. New way to map old sutures using deformed alkaline rocks and carbonatites. *Geology*. 2003. Vol. 31. N 5, p. 391-394. DOI: 10.1130/0091-7613(2003)031<0391:NWTMOS>2.0.CO;2

10. Attoh K., Corfu F., Nude P.M. U-Pb zircon age of deformed carbonatite and alkaline rocks in the Pan-African Dahomeyide suture zone,West Africa. *Precambrian Research*. 2007. Vol. 155. Iss. 3-4, p. 251-260. DOI: 10.1016/j.precamres.2007.02.003

11. Emmanuel N.N., Rigobert T., Nédélec A. et al. Structure and petrology of Pan-African nepheline syenites from the South West Cameroon; Implications for their emplacement mode, petrogenesis and geodynamic significance. *Journal of African Earth Sciences*. 2013. Vol. 87, p. 44-58. DOI: 10.1016/J.JAFREARSCI.2013.07.008

12. Valentin E., Botelho N.F., Dantas E.L. Monte Santo suite, an example of Ediacaran-Cambrian deformed alkaline rocks in the Araguaia Belt, Central Brazil. Implications for Western Gondwana evolution. *Lithos*. 2020. Vol. 366. N 105552. DOI: 10.1016/j.lithos.2020.105552

13. Kramm U., Blaxland A.B., Kononova V.A., Grauert B.J. Origin of the Ilmenogorsk-Vishnevogorsky nepheline syenites, Urals, USSR, and their time of emplacement during the history of the Ural fold belt: A Rb-Sr study. *Geology*. 1983. Vol. 91. N 4, p. 427-435. DOI: 10.1086/628788

14. Levin V.Ya., Ronenson B.M., Samkov V.S. et al. Alkaline-carbonatite complexes of the Urals. Ekaterinburg: Uralgeolkom, 1997, p. 271 (in Russian).

15. Abramov S.S., Rass I.T., Kononkova N.N. Fenites of the Miaskite-Carbonatite Complex in the Vishnevye Mountains, South Urals, Russia: Origin of the Metasomatic Zoning and Thermodynamic Simulations of the Processes. *Petrology*. 2020. Vol. 28. N 3, p. 263-286. DOI: 10.1134/S0869591120030029

16. Mitchell R.H. Carbonatites, and carbonatites and carbonatites. *Canadian Mineralogist*. 2005. Vol. 43. N 6, p. 2049-2068. DOI: 10.2113/gscanmin.43.6.2049

17. Ivanov K.S. The genesis of carbonatites of the Urals. *Lithosphere (Russia)*. 2011. N 1, p. 20-33 (in Russian).

18. Puchkov V.N. Geology of the Urals and Cis-Urals (topical issues of stratigraphy, tectonics, geodynamics, and metallogeny). Ufa: DizaynPoligrafServis, 2010, p. 280 (in Russian).

19. Nedosekova I.L., Belyatsky B.V. Age and substance sources of the Ilmeno-Vishnevogorsky Alkaline Complex (South Urals): Rb-Sr, Sm-Nd, U-Pb, and Lu-Hf isotope data. *Doklady Earth Sciences*. 2012. Vol. 446. Part 1, p. 1071-1076. DOI: 10.1134/S1028334X12090061

20. Krasnobaev A.A., Busharina S.V., Valizer P.M., Medvedeva E.V. Zirconology of miaskites of the Ilmeny Mountains (South Urals). *Geochemistry International*. 2016. Vol. 54, p. 765-780. DOI: 10.1134/S0016702916070041

21. Krasnobaev A.A., Valizer P.M., Rusin A.I. et al. Zirconology of ultramafic rocks of the Buldym Massif (Il'meno-Vishnevogorskii Complex, South Urals). *Doklady Earth Sciences*. 2015. Vol. 461, p. 235-241. DOI: 10.1134/S1028334X15030022

22. Chernyshev I.V., Kononova V.A., Kramm U., Grauert B. Isotope geochronology of alkaline rocks of the Urals in the light of uranium-lead data for zircons. *Geokhimiya*. 1987. N 3, p. 323-338 (in Russian).

23. Krasnobaev A.A., Rusin A.I., Valizer P.M., Busharina S.V. Zirconology of calcite carbonatite of the Vishnevogorsky Massif, South Urals. *Doklady Earth Sciences*. 2010. Vol. 431, p. 390-393. DOI: 10.1134/S1028334X10030268

24. Nedosekova I.L., Belyatsky B.V., Belousova E.A. Trace elements and Hf isotope composition as indicators of zircon genesis in the evolution of the alkaline-carbonatite magmatic system (Ilmeno-Vishnevogorsky complex, Urals, Russia). *Russian Geology and Geophysics*. 2016. Vol. 57. Iss. 6, p. 891-906. DOI: 10.1016/j.rgg.2015.09.021

25. Nedosekova I.L., Belousova E.A., Sharygin V.V. Sources of matter of the Ilmeno-Vishnevogorsky alkaline complex according to Lu-Hf isotopy data for zircons. *Doklady Earth Sciences*. 2010. Vol. 435. N 2, p. 234-239 (in Russian).

26. Valizer P.M., Nemov A.B., Krasnobaev A.A. et al. Zirconology of Pegmatites of the Ilmeny Mountains. *Doklady Earth Sciences*. 2014. Vol. 457. N 2, p. 960-964. DOI: 10.1134/S1028334X14080066

27. Belyatsky B.V., Lepekhina E.N., Antonov A.V. et al. The Age of Nb Rare-Metal Mineralization of the Ilmeny-Vishnevogorsky Alkaline Complex (South Urals). *Doklady Earth Sciences*. 2018. Vol. 481. N 2, p. 1079-1085. DOI: 10.1134/S1028334X18080251

28. Popova V.I., Popov V.A., Blinov I.A. et al. New findings of rare minerals in pegmatites of vishnevye mountains in the South Urals. *Minerals*. 2019. N 1, p. 1-14 (in Russian).

29. Nedosekova I.L., Ronkin Yu.L., Lepikhina O.P. New data on carbonatites of the Ilmeno-Vishnevogorsky complex (South Urals, Russia). *Geologiya rudnykh mestorozhdeniy*. 2007. Vol. 49. N 2, p. 146-164 (in Russian).

30. Popov V.A., Rassomakhin M.A., Kolisnichenko S.V. A Unique Ore Locality of Polyakovite-(Ce) in the Ilmeny Mountains, South Urals – New Finds. *Minerals*. 2020. Vol. 6. N 1, p. 17-32 (in Russian). DOI: 10.35597/2313-545X-2020-6-1-2

31. Woolley A.R., Kempe D.R.C., Bell K. Carbonatites: Nomenclature, average compositions, and element distribution. Carbonatites: Genesis and Evolution. London: Unwin Hyman, 1989, p. 1-14.

32. Le Maitre R.W. Igneous Rocks: A classification and Glossary of Terms. Cambridge: Cambridge University Press, 2002, p. 236.

33. Nedosekova I.L., Vladykin N.V., Pribavkin S.V., Bayanova T.B. Ilmeno-Vishnevogorsky miaskite-carbonatite complex: Origin, ore content, sources of substance (Ural, Russia). *Geology of Ore Deposits*. 2009. Vol. 51, p. 157-181. DOI: 10.1134/S1075701509020056

34. Levashova E.V., Skublov S.G., Popov V.A. Distribution of trace elements controlled by sector and growth zonings in zircon from feldspathic pegmatites (Ilmen Mountains, the South Urals). *Geosciences*. 2021. Vol. 11. Iss. 1. N 7. DOI: 10.3390/geosciences11010007

35. Kasatkin A.V., Škoda R., Nestola F. et al. Röentgenite-(Ce) and other ree fluorcarbonates from vein N 35, Vishnevye mountains, South Urals. *Minerals*. 2019. N 5, p. 10-22 (in Russian). DOI: 10.35597/2313-545X-2019-5-2-10-22

36. Popova V.I., Popov V.A., Blinov I.A., Kotlyarov V.A. New Data on Pyrochlore of Alkali Pegmatites And Ore Zones of the Vishnevye Mountains (South Urals). *Minerals*. 2018. Vol. 4, N 3, p. 46-60 (in Russian).

37. Atencio D., Andrade M.B., Christy A.G. et al. The pyrochlore supergroup of minerals: nomenclature. *Canadian Mineralogist*. 2010. Vol. 48. N 3, p. 673-698. DOI: 10.3749/canmin.48.3.67

38. Hogarth D.D. Classification and nomenclature of the pyrochlore group. *American Mineralogist*. 1977. Vol. 62, p. 403-410.

39. Kozlov E., Fomina E., Sidorov M. et al. Ti-Nb Mineralization of Late Carbonatites and Role of Fluids in Its Formation: Petyayan-Vara Rare-Earth Carbonatites (Vuoriyarvi Massif, Russia). *Geosciences (Switzerland)*. 2018. Vol. 8. Iss. 8. N 281. DOI: 10.3390/geosciences8080281

40. Burke K., Khan S. Geoinformatic approach to global nepheline syenite and carbonatite distribution: Testing a Wilson cycle model. *Geosphere*. 2006. Vol. 2. Iss. 1, p. 53-60. DOI: 10.1130/GES00027.1

41. Upadhyay D., Raith M.M., Mezger K. et al. Mesoproterozoic rifting and Pan-African continental collision in SE India: evidence from the Khariar alkaline complex. *Contributions to Mineralogy and Petrology*. 2006. Vol. 151. Iss. 4, p. 434-456. DOI: 10.1007/s00410-006-0069-4

42. Eby G.N., Woolley A.R., Din V.I.C., Platt G.J. Geochemistry and Petrogenesis of Nepheline Syenites: Kasungu – Chipala, Ilomba, and Ulindi Nepheline Syenite Intrusions, North Nyasa Alkaline Province, Malawi. *Petrology*. 1998. Vol. 39. Iss. 8, p. 1405-1424. DOI: 10.1093/petroj/39.8.1405

43. Arzamastsev A.A., Bea F., Glaznev V.N. et al. Kola alkaline province in the Palaeozoic: Evaluation of primary mantle magma composition and magma generation conditions. *Russian Journal Earth Science*. 2001. N 3, p. 1-32.

44. Sørensen H. Development of Nepheline Syenites in Rift Zones – Information from three Rift Complexes. *GeoLines*. 2003. Vol. 15. p. 140-146.

45. Wang K., Plank T., Walker J.D., Smith E.I. A mantle melting profile across the Basin and Range, SW USA. *Journal of Geophysical Research*. 2002. Vol. 107. Iss. B1. N ECV 5-1-ECV 5-21. DOI: 10.1029/2001JB000209

46. Casquet C., Pankhurst R.J., Galindo C. et al. A deformed alkaline igneous rock–carbonatite complex from the Western Sierras Pampeanas, Argentina: Evidence for late Neoproterozoic opening of the Clymene Ocean? *Precambrian Research*. 2008. Vol. 165. Iss. 3-4, p. 205-220. DOI: 10.1016/j.precamres.2008.06.011

47. Das S., Sanyal S., Karmakar S. et al. Do the deformed alkaline rocks always serve as a marker of continental suture zone? A case study from parts of the Chotanagpur Granite Gneissic complex, India. *Journal of Geodynamics*. 2018. Vol. 129, p. 59-79. DOI: 10.1016/j.jog.2018.10.001

48. Zengqian Houa, Shihong Tian, Zhongxin Yuan et al. The Himalayan collision zone carbonatites in western Sichuan, SW China: petrogenesis, mantle source and tectonic implication. *Earth and Planetary Science Letters*. 2006. Vol. 244, p. 234-250. DOI: 10.1016/j.epsl.2006.01.052

49. Khromova E.A., Doroshkevich A.G., Izbrodin I.A. Geochemical and Sr-Nd-Pb Isotopic Characteristics of Alkaline Rocks and Carbonatite Of The Belaya Zima Massif (Eastern Sayan). *Geosphere Research*. 2020. N 1, p. 33-55 (in Russian). DOI: 10.17223/25421379/14/3

50. Downes H., Balaganskaya E., Beard A., Liferovich R. Petrogenetic processes in the ultramafic, alkaline and carbonatitic magmatism in the Kola Alkaline Province: A review. *Lithos*. 2005. Vol. 85. Iss. 1-4, p. 48-75. DOI: 10.1016/j.lithos.2005.03.020

51. Arzamastsev A.A., Mitrofanov F.P. Paleozoic Plume-Lithospheric Processes in Northeastern Fennoscandia: Evaluation of the Composition of the Parental Mantle Melts and Magma Generation Conditions. *Petrology*. 2009. Vol. 17. N 3, p. 300-313. DOI: 10.1134/S0869591109030060

52. Chakhmouradian A.R., Reguir E.P., Kressall R.D. et al. Carbonatite-hosted niobium deposit at Aley, northern British Columbia (Canada): Mineralogy, geochemistry and petrogenesis. *Ore Geology Reviews*. 2015. Vol. 64, p. 642-666. DOI: 10.1016/j.oregeorev.2014.04.020

53. Sorokina E.S., Botcharnikov R.E., Kostitsyn Y.A. et al. Sapphire-bearing magmatic rocks trace the boundary between paleo-continents: A case study of Ilmenogorsky alkaline complex, Uralian collision zone of Russia. *Gondwana Research*. 2021. Vol. 92, p. 239-252. DOI: 10.1016/j.gr.2021.01.001

54. Marin Y.B. On mineralogical studies and the use of mineralogical information in solving petro- and ore genesis problems. *Geology of Ore Deposits*. 2021. Vol. 63, p. 625-633. DOI: 10.1134/S1075701521070059

55. Akbarpuran H.S.A., Gulbin Y.L., Sirotkin A.N., Gembitskaya I.M. Compositional evolution of REE- and Ti-bearing accessory minerals in metamorphic schists of atomfjella series, western ny friesland, svalbard and its petrogenetic significance. *Geology of Ore Deposits*. 2021. Vol. 63, p. 634-653. DOI: 10.1134/S1075701521070047

56. Guzev V.E., Terekhov A.V., Skublov S.G. et al. The first data on the U-Pb ages and compositions of zircons from ore-bearing syenites of gora Rudnaya (South Yakutia). *Russian Journal of Pacific. Geology*. 2021. Vol. 15, p. 570-582. DOI: 10.1134/S1819714021060038

57. Skublov S.G., Li S.-K. Anomalous geochemistry of zircon from the Yastrebetskoe rare metal deposit (SIMS- and TOF-study). *Journal of Mining Institute*. 2016. Vol. 222, p. 798-802. DOI: 10.18454/PMI.2016.6.798

58. Sergeeva L.Y., Berezin A.V., Gusev N.I. et al. Age and metamorphic conditions of the granulites from Capral-Jegessky synclinoria, Anabar shield. *Journal of Mining Institute*. 2018. Vol. 229, p. 13-21. DOI: 10.25515/PMI.2018.1.13

59. Yatsenko I.G., Skublov S.G., Levashova E.V. et al. Composition of spherules and lower mantle minerals, isotopic and geochemical characteristics of zircon from volcaniclastic facies of the Mriya lamproite pipe. *Journal of Mining Institute*. 2020. Vol. 242, p. 150-159. DOI: 10.31897/PMI.2020.2.150

Author **Irina L. Nedosekova**, *Candidate of Geological and Mineralogical Sciences, Leading Researcher, vladi49@yandex.ru, https://orcid.org/0000-0001-7952-0639 (Zavaritsky Institute of Geology and Geochemistry, the Ural Branch of the Russian Academy of Sciences, Yekaterinburg, Russia)*